DNA Electrokinetic Translocation through a Nanopore: Local Permittivity Environment Effect

ARTICLE *in* THE JOURNAL OF PHYSICAL CHEMISTRY C · FEBRUARY 2012

Impact Factor: 4.77 · DOI: 10.1021/jp211798x

THE JOURNAL OF PHYSICAL CHEMISTRY C

Article

pubs.acs.org/JPCC

DNA Electrokinetic Translocation through a Nanopore: Local Permittivity Environment Effect

Mingkan Zhang,[†,∥] Li-Hsien Yeh,[†,‡,∥] Shizhi Qian,*[,†,§] Jyh-Ping Hsu,*[,‡] and Sang W. Joo[§]

[†]Institute of Micro/Nanotechnology, Old Dominion University, Norfolk, Virginia 23529, United States

[‡]Department of Chemical Engineering, National Taiwan University, Taipei, 10617, Taiwan

[§]School of Mechanical Engineering, Yeungnam University, Gyongsan 712-719, South Korea

Supporting Information

ABSTRACT: The effect of the local liquid permittivity surrounding the DNA nanoparticle, referred to as the local permittivity environment (LPE) effect, on its electrokinetic translocation through a nanopore is investigated for the first time using a continuum-based model, composed of the coupled Poisson−Nernst−Planck (PNP) equations for the ionic mass transport and the Stokes and Brinkman equations for the hydrodynamic fields in the region outside of the DNA and within the ion-penetrable layer of the DNA nanoparticle, respectively. The nanoparticle translocation velocity and the resulting current deviation are systematically investigated for both uniform and spatially varying permittivities surrounding the DNA nanoparticle under various conditions. The LPE effect in general reduces the particle translocation velocity. The LPE effect on the current deviation is insignificant when the imposed electric field is relatively high. However, when the electric field and the bulk electrolyte concentration are relatively low, both current blockade and enhancement are predicted with the LPE effect incorporated, while only current blockade is predicted with the assumption of constant liquid permittivity. It is thereby shown that regardless of the electric field imposed the predictions on ionic current with considering the LPE effect are in good qualitative agreement with the experimental observations obtained in the literature.

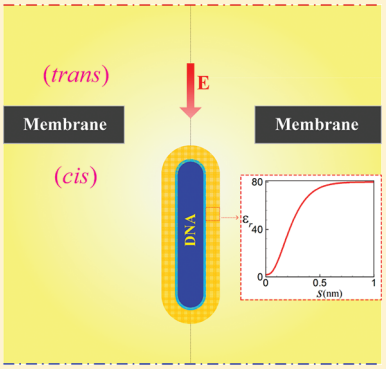

1. INTRODUCTION

Solid-state nanopores[1] have emerged as single-molecule biosensors for detection and characterization of biopolymers, such as polypeptide,[2,3] RNA,[4] and DNA,[4−6] over the past decade. Electrically driven charged nanoparticle translocation through a nanopore giving rise to detectable changes in the ionic current enables sensing of unlabeled single molecules for various bioanalytical applications. Among these, the nanopore-based DNA sequencing technique[7−9] is one of the most promising applications, which makes it possible to identify the nucleotide bases sequence by discriminating the ionic current signals at high speed and low lost.[8]

With the inception of nanopore-based sensing techniques, a growing number of experimental[2,3,5,9−20] and theoretical studies[20−31] on single-molecule sensors have appeared. Experimental results demonstrated that the ionic current during the DNA translocation depends on the thickness of the membrane,[5,16] the pore materials and radius,[5,14,16−18] the DNA length,[5,11,13,14,20] the voltage imposed across the nanopore,[10,17] and the pH[19] and the bulk concentration[11,12,15] of the aqueous solution. When bulk salt concentration is relatively high (e.g., 1 M) the current blockade[5,9,10,13−20] is observed typically during the single-molecule translocation. Chang et al.[11] first found that when the bulk salt concentration is relatively low (e.g., 0.1 M) and the DNA length is comparable to the thickness of the nanopore membrane the surprising current enhancement appears. Later, Fan et al.[32] found that the current blockade and the current enhancement phenomena during the DNA translocation through inorganic nanotubes depend on the buffer concentration. Dekker's group[12] further demonstrated the dependence of the ionic current on the salt concentration in solid-state nanopores, which was analyzed numerically more recently by He et al.[30] with the Poisson−Boltzmann coupled with Navier−Stokes equations. Both the current blockade and current enhancement phenomena during the DNA translocation through nanopores are predicted by Timp's[22] and Schulten's group[21] as well by using the molecular dynamics (MD) simulations. Liu et al.[25] later adopted the coupled Poisson−Nernst−Planck (PNP) with Navier−Stokes (NS) equations to theoretically investigate the problem and concluded that their results based on the PNP coupled with NS model are successful in predicting ionic current through a nanopore and in good qualitative agreement with the experimental data and MD simulations.

All of the aforementioned theoretical predictions for ionic current during the electrokinetic DNA translocation through nanopores are based on a general assumption of constant liquid permittivity inside and outside the DNA molecules. Many existing observations, however, indicate that this basic assumption of constant liquid permittivity is unrealistic and incorrect.[33−37]

Received: December 7, 2011
Revised: January 19, 2012
Published: January 23, 2012

   dx.doi.org/10.1021/jp211798x | J. Phys. Chem. C 2012, 116, 4793−4801

In the vicinity of a charged DNA molecule in water, the local liquid permittivity in fact deviates obviously from its bulk value as a consequence of the significant counterion condensation and the strong hydrogen bonding interactions.[33,36] Consequently, the activity of the water and ions as well as the local liquid permittivity surrounding the DNA are reduced. On the basis of fitting to the local permittivity obtained from the MD simulations, the spatially varying permittivity from the DNA nanoparticle surface ε_r, referred to as the local permittivity environment (LPE) effect, can be described by the empirical Hingerty–Lavery type sigmoidal function[34,35]

$$\varepsilon_r = \varepsilon_w - \left[\left(\frac{\varepsilon_w - \varepsilon_i}{2}\right)(\alpha^2 + 2\alpha + 2)e^{-\alpha}\right] \quad (1)$$

Here $\varepsilon_w = 80$ and $\varepsilon_i = 1.76$ are the relative permittivity of the liquid phase far away (bulk aqueous solution) and on the DNA nanoparticle surface, respectively, and $\alpha = 1.2s$, with s being the normal distance from the DNA surface. The inset of Figure 1

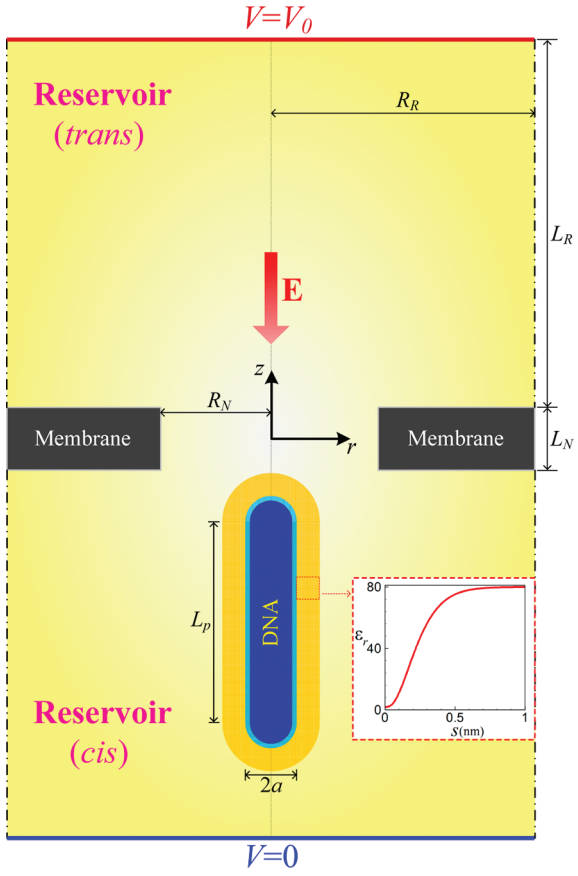

Figure 1. Schematic view of a soft DNA translocation through a nanopore. Inset: variation of the local permittivity environment as a function of the normal distance from the DNA surface based on eq 1.[35]

depicts the local liquid permittivity as a function of the normal distance from the DNA nanoparticle surface, and ε_r significantly varies from $\varepsilon_i = 1.76$ to $\varepsilon_w = 80$ in a region of about 1 nm from the DNA surface.

In the present study, by taking into account the LPE effect for the first time, the DNA electrokinetic translocation through a nanopore is investigated using a continuum-based model, composed of the coupled Poisson–Nernst–Planck (PNP) equations for the ionic mass transport and the Stokes and Brinkman equations[38−41] for the hydrodynamic fields in the region outside of the DNA and within the ion-penetrable layer of the DNA nanoparticle, respectively. The nanoparticle translocation velocity and the resulting current deviation for both constant and spatially varying permittivities surrounding the DNA nanoparticle are examined in detail by varying the bulk ionic concentration, the strength of the applied electric field, and the nanopore surface charge density. We will conclude, for the first time, that regardless of the electric field imposed the predictions on ionic current with the LPE effect included are in good qualitative agreement with the experimental observations in the literature. This study is also aimed to provide theoretical background for elaboration of the physical mechanisms of controlling the DNA translocation through a nanopore.

2. MATHEMATICAL MODEL

We consider a nanopore of length L_N and radius R_N connecting two large, identical reservoirs (referred to as *cis* and *trans* reservoirs, respectively) of length L_R and radius R_R on either side, as schematically shown in Figure 1. The nanopore and reservoirs are filled with an aqueous binary electrolyte solution with z_1 and z_2 being the valences of the cations and the anions, respectively. A double-stranded DNA (dsDNA) molecule is initially positioned inside the *cis* reservoir as shown in Figure 1. The dsDNA contains a rigid inner core, which is approximated as an uncharged nanorod of length L_p with two hemispheres of radius a on either end, covered by an ion-penetrable soft layer of uniform thickness d.[25,37] The ion-penetrable soft layer is homogeneously structured and bears dissociable function groups to form the phosphate backbones in DNA, yielding a uniform fixed charge density, ρ_{fix}, and an extra friction force acting on the liquid flowing inside.[38] We further assume that the DNA nanoparticle is initially placed with its axis coinciding with the cylindrical nanopore's axis so that a two-dimensional axial symmetric geometry can be used to describe all variables in the present study. The origin of the cylindrical coordinate (r, z) is fixed at the center of the nanopore. The two reservoirs are assumed large enough for the ionic concentration far away from the nanopore to maintain its bulk value, C_0. A potential bias V_0 is applied between the two electrodes positioned far away from the nanopore inside the two reservoirs, inducing a negative axial electric field, **E**, to electrophoretically drive the negatively charged DNA from the *cis* reservoir along the axis of the nanopore toward the *trans* reservoir and simultaneously generate a detectable ionic current through the nanopore.

In the present study, we adopt the verified continuum-based model, composed of the PNP equations for the ionic mass transport and the Stokes equations for the hydrodynamic field,[38−41] to model the DNA electrokinetic translocation through a nanopore with the emphasis on the LPE effect. The ionic mass transport in the electrolyte solution is governed by the PNP equations[27,41]

$$-\nabla\cdot(\varepsilon_0\varepsilon_{f,i}\nabla V) = \rho_e + \rho_{fix}, \quad \text{inside the ion-penetrable layer} \quad (2)$$

$$-\nabla\cdot(\varepsilon_0\varepsilon_{f,o}\nabla V) = \rho_e, \quad \text{outside the ion-penetrable layer} \quad (3)$$

dx.doi.org/10.1021/jp211798x | J. Phys. Chem. C 2012, 116, 4793−4801

and

$$\nabla\cdot\mathbf{N}_j = \nabla\cdot\left(\mathbf{u}c_j - D_j\nabla c_j - z_j\frac{D_j}{RT}Fc_j\nabla V\right) = 0,\ j = 1 \text{ and } 2 \tag{4}$$

In the above, V is the electric potential; $\mathbf{u}$ is the fluid velocity; $\rho_e = F(z_1c_1 + z_2c_2)$ is the space charge density of mobile ions; $\mathbf{N}_j$, c_j, D_j, and z_j are the ionic flux density, the ionic concentration, the diffusivity, and the valence of the jth ionic species, respectively (j = 1 and 2 represent the cations and anions, respectively); ε_0, F, R, and T are the vacuum permittivity, the Faraday constant, the universal gas constant, and the absolute temperature, respectively; and $\varepsilon_{f,i}$ and $\varepsilon_{f,o}$ are the relative permittivities of the liquid phase inside and outside the ion-penetrable layer, respectively.

Since the Reynolds number of the electrokinetic flow in nanofluidics is extremely low (i.e., Re $\ll$ 1), the flow field at the quasi-steady state can be described by the modified Stokes equations[38−41]

$$-\nabla p + \mu\nabla^2\mathbf{u} - F(z_1c_1 + z_2c_2)\nabla V - \gamma(\mathbf{u} - \mathbf{u}_p) = 0, \text{ inside the ion-penetrable layer} \tag{5}$$

$$-\nabla p + \mu\nabla^2\mathbf{u} - F(z_1c_1 + z_2c_2)\nabla V = 0, \text{ outside the ion-penetrable layer} \tag{6}$$

and

$$\nabla\cdot\mathbf{u} = 0 \tag{7}$$

In the above, p and μ are the hydrodynamic pressure and the dynamic viscosity of the fluid, respectively; γ is the hydrodynamic frictional coefficient of the ion-penetrable layer; $\mathbf{u}_p = U_p\mathbf{e}_z$ is the particle translocation velocity along the axis of the nanopore; and $\mathbf{e}_z$ is the unit vector in the z-direction.

To solve the above coupled governing equations, eqs 2−7, appropriated boundary conditions are required. The ionic concentrations at the ends of the two reservoirs are the bulk ionic concentrations, $c_j = C_{j0}$, where j = 1 and 2. The particle's rigid core is ion-impermeable. Since the particle is translating with a velocity, U_p, along the axis of the nanopore, the normal ionic flux at the surface of the rigid core includes the convective flux, $\mathbf{n}\cdot\mathbf{N}_j = \mathbf{n}\cdot(\mathbf{u}c_j)$, j = 1 and 2, where $\mathbf{n}$ is the unit normal vector directed from the corresponding surface into the fluid.[42] At the ion-penetrable layer/liquid interface of the DNA nanoparticle, the concentration and normal flux of each ionic species are continuous. The normal ionic fluxes on all other boundaries are zero.

For the electric field, the electric potential imposed at the ends of the *cis* and *trans* reservoirs are $V = 0$ and $V = V_0$, respectively. The surface of the particle's rigid core is assumed uncharged, $-\mathbf{n}\cdot(\varepsilon_0\varepsilon_{f,i}\nabla V) = 0$.[38] The surface charge density on the nanopore wall is specified as $-\mathbf{n}\cdot(\varepsilon_0\varepsilon_{f,o}\nabla V) = \sigma_w$, and all other boundaries use the insulating boundary condition, $-\mathbf{n}\cdot(\varepsilon_0\varepsilon_{f,o}\nabla V) = 0$. At the ion-penetrable layer/liquid interface of the DNA nanoparticle, the continuous boundary condition for the electric potential and the normal electric field is used.

For the flow field, a nonslip boundary condition is imposed on the inner surfaces of the nanopore and the membrane. A normal flow with no external pressure gradient (i.e., $p = 0$) is applied at the ends of the two big reservoirs. Since the side boundaries of the two reservoirs are far away from the nanopore, a symmetric slip boundary condition is specified. Along the ion-penetrable layer/liquid interface of the DNA, a continuous flow boundary condition, including the flow velocity and both the normal and the tangential viscous stress tensors, is used.[38] As the DNA translocates along the axis of the nanopore, the fluid velocity on the surface of the particle's rigid core is $\mathbf{u} = U_p\mathbf{e}_z$. Under the quasi-steady state, the particle translocation velocity, U_p, will be determined by the condition of zero net force acting on the particle[27,41]

$$F_E + F_H = 0 \tag{8}$$

where F_E and F_H are, respectively, the z-component electrical and hydrodynamic forces acting on the particle, and they are obtained by the integration of the Maxwell stress tensor[27,41] and the hydrodynamic stress tensor,[27,38,41] over the DNA nanoparticle surface Ω_p, respectively

$$F_E = \int_{\Omega_p}\varepsilon_0\varepsilon_{f,o}\left[\frac{\partial V}{\partial r}\frac{\partial V}{\partial z}n_r - \frac{1}{2}\left(\left(\frac{\partial V}{\partial r}\right)^2 + \left(\frac{\partial V}{\partial z}\right)^2\right)n_z\right]d\Omega_p \tag{9}$$

and

$$F_H = \int_{\Omega_p}\left[\mu\left(\frac{\partial u_r}{\partial z} + \frac{\partial u_z}{\partial r}\right)n_r + n_z\left(-p + 2\mu\frac{\partial u_z}{\partial z}\right)\right]d\Omega_p \tag{10}$$

In the above, n_r and n_z are the r- and z-components of the unit normal vector, $\mathbf{n}$, respectively, and u_r and u_z are, respectively, the r- and z-components of the fluid velocity.

In experiments, one typically measures the ionic current flowing through the nanopore as a function of time during the DNA nanoparticle translocation process. The ionic current is evaluated by

$$I = \int_S F\left(\sum_{j=1}^{2} z_j\mathbf{N}_j\right)\cdot\mathbf{n}dS \tag{11}$$

where S denotes either end of the reservoirs due to the ionic current conservation. To measure the effect of the translocating DNA nanoparticle on the ionic current through the nanopore, ionic current deviation is defined as

$$\chi = \frac{I - I_\infty}{I_\infty} \tag{12}$$

where I_∞ is the base ionic current when the DNA nanoparticle is far away from the nanopore. $\chi < 0$ represents a current blockade, while $\chi > 0$ implies a current enhancement during the translocation process. In the following, we will present many of our results in the form of the particle translocation velocity and χ as a function of the particle's location (i.e., center of mass), z_p.

The dimensionless form of the above mathematical model can be easily derived using the bulk concentration C_0 as the ionic concentration scale, the radius of the dsDNA nanoparticle a as the length scale, RT/F as the potential scale, $U_0 = \varepsilon_0\varepsilon_w R^2T^2/(\mu aF^2)$ as the velocity scale, and $\mu U_0/a$ as the pressure scale. ε_w is the relative permittivity of water.

3. RESULTS AND DISCUSSION

The strongly coupled dimensionless mathematical model is numerically solved with the commercial finite element package, COMSOL Multiphysics (version 3.5a, www.comsol.com),

dx.doi.org/10.1021/jp211798x | J. Phys. Chem. C 2012, 116, 4793−4801

installed in a high-performance cluster. To capture the EDLs in the vicinity of the charged particle and nanopore wall, sufficient mesh is generated around the particle and near the nanopore wall. All the results presented in this study are ensured to be convergent and mesh-independent. The details of the numerical implementation and the code validation can be found in the Supporting Information.

In the present study, we assume the radius of the dsDNA nanoparticle is a = 1.1 nm[11] and the thickness of its ion-penetrable layer is 0.3 nm, which corresponds to the hydrodynamic diameter of the water molecule.[43] Because one helical pitch of the dsDNA has about 10.5 base pairs (bp)[44] and one bp carries two elementary charges and has a length of 0.334 nm,[45] the fixed charge density of the DNA nanoparticle ρ_{fix} is estimated as -6×10^7 C/m^3 by dividing the bare charge density of $\rho_{fix,b} = -2.53 \times 10^8$ C/m^3 by the Manning factor of 4.2.[46,47] The bare fixed charge density corresponds to the typical value of the linear charge density on the DNA (ca. six elementary charges/nanometer). The total length of the DNA nanoparticle L_p is assumed to be 49 nm (ca. 14 helical pitch), which is less than the persistence length of the dsDNA (ca. 50 nm)[47] to ensure it is a reasonable approximation by a cylindrical nanorod with two hemispheres on both ends. Since the DNA can be viewed as a highly charged polyelectrolyte, the counterion condensation occurs, resulting in lots of counterions accumulated in the vicinity of the DNA.[36,46,47] The counterion condensation effect strongly reduces the activity of the ions near the DNA and accordingly decreases the local liquid permittivity surrounding the DNA,[36,48] which is referred to as the LPE effect in the present study. Similarly, counterion condensation also occurs in the vicinity of the charged nanopore wall, inducing the LPE effect near the charged nanopore wall. We focus on the LPE effect only arising from the counterion condensation of the DNA and assume that the LPE effect stemming from the charged nanopore wall is neglected in the present study. Without considering the LPE effect, the relative permittivity of the liquid within the soft layer and outside of the DNA is a constant, $\varepsilon_{f,i} = \varepsilon_{f,o} = \varepsilon_w = 80$. When the LPE effect arising from the charged DNA is considered, spatially varying relative permittivity is used, $\varepsilon_{f,i} = \varepsilon_i$ and $\varepsilon_{f,o} = \varepsilon_r$, which is defined in eq 1. We assume the system is filled with KCl aqueous solution. The physical parameters used in the present study are summarized in Table 1.

Figure S2 in the Supporting Information depicts the normalized particle translational velocity, U_p/U_0, when the DNA is located at the center of the nanopore as a function of the hydrodynamic frictional coefficient of the ion-penetrable layer of the DNA, γ. The particle velocity decreases rapidly with increasing γ and saturates when the latter exceeds a certain critical value, γ_{cr}. To ensure that the DNA maintains an elongated structure during the whole translocation process, we choose $\gamma = 1.32 \times 10^{18}$ kg/sm^3, which is much higher than γ_{cr}, in the followings simulations.

3.1. EFFECT OF THE BULK IONIC CONCENTRATION

Figure 2 depicts the normalized translational velocity of the DNA nanoparticle (Figure 2a) and the resulting ionic current deviation (Figure 2b) as a function of the particle's location, z_p, for various bulk ionic concentrations. Solid lines with symbols represent the results without considering the LPE effect ($\varepsilon_{f,i} = \varepsilon_{f,o} = \varepsilon_w = 80$), while lines without symbols represent the results with the LPE effect ($\varepsilon_{f,i} = \varepsilon_i$ and $\varepsilon_{f,o} = \varepsilon_r$). Since the electric field inside the nanopore is higher than that in the fluid reservoirs, as expected the particle velocity within the nanopore is higher than that inside the fluid reservoirs. This phenomenon is consistent with many theoretical and experimental observations in the literature.[25,27−29,49] Under the other same conditions, the particle velocities with the LPE effect are lower than those without considering the LPE effect. Compared to the case without LPE effect, more counterions are confined near the DNA surface in the presence of the LPE effect, resulting in lower effective charge density, $\rho_e + \rho_{fix}$, accumulated within the soft layer of the DNA particle and accordingly lower particle electrophoretic velocity. It is interesting to note that the maximum particle translational velocity does not occur when the particle is at the center of the nanopore, and the particle velocity peaks at about $z_p = \pm 15.6$ nm, at which the front (rear) end of the DNA nanoparticle reaches the edge of the nanopore at the *trans* (*cis*) reservoir. When the particle is completely inside the nanopore, the particle velocity decreases in the range of -15.6 nm $< z_p < 0$ and increases in the range of $0 < z_p < 15.6$ nm. Without considering the LPE effect, the first peak particle velocity occurring at about $z_p = -15.6$ nm is lower than the second peak particle velocity occurring at $z_p = 15.6$ nm when the bulk ionic concentration is relatively low (i.e., $C_0 = 10$ mM), and the particle velocity is almost symmetric with respect to $z_p = 0$ when the bulk ionic concentration is relatively high (i.e., $C_0 = 100$ and 1000 mM). However, for the case of considering the LPE effect, the first peak particle velocity is always higher than the second peak particle velocity, and the particle velocity is not symmetric with respect to $z_p = 0$. The asymmetric particle velocity profile can be attributed to the competitive effects of the enhanced local electric field inside the nanopore[31,50] and the induced concentration polarization (CP), as schematically illustrated in Figure 3. The enhancement of the local electric field inside the nanopore arises from the large mismatch of the cross-sectional areas of the fluid reservoirs and the nanopore,[50] resulting in higher particle velocity inside the nanopore. The CP effect is induced by the flow in the gap between the particle

Table 1. Values or Range of the Parameters Used in the Present Study

parameters	value or range
a (DNA radius)	1.1 (nm)
L_p (DNA length)	49 (nm)
R_N (nanopore radius)	3 (nm)
L_N (nanopore length)	20 (nm)
R_R (reservoir radius)	260 (nm)
L_R (reservoir length)	250 (nm)
d (thickness of ion-penetrable layer of DNA)	0.3 (nm)
ε_w (relative permittivity of water)	80
ε_i (relative permittivity of liquid on DNA surface)	1.76
ε_0 (vacuum permittivity)	8.854×10^{-12} (C/Vm)
μ (dynamic viscosity)	0.001 (kg/sm)
ρ (fluid density)	1000 (kg/m^3)
F (Faraday constant)	96490 (C/mol)
c_0 (bulk ionic concentration)	10−1000 (mM)
γ (friction coefficient of ion-penetrable layer)	1.32×10^{18} (kg/sm^3)
ρ_{fix} (fixed charge density of ion-penetrable layer)	-6×10^7 (C/m^3)
D_1 (diffusion coefficient of cations)	1.957×10^{-9} (m^2/s)
D_2 (diffusion coefficient of anions)	2.032×10^{-9} (m^2/s)
T (absolute temperature)	300 (K)
R (universal gas constant)	8.31 (1/mol K)
E (strength of applied electric field)	20 or 2000 (kV/m)
σ_w (charge density on nanopore wall)	0 or −0.009 (C/m^2)

dx.doi.org/10.1021/jp211798x | J. Phys. Chem. C 2012, 116, 4793−4801

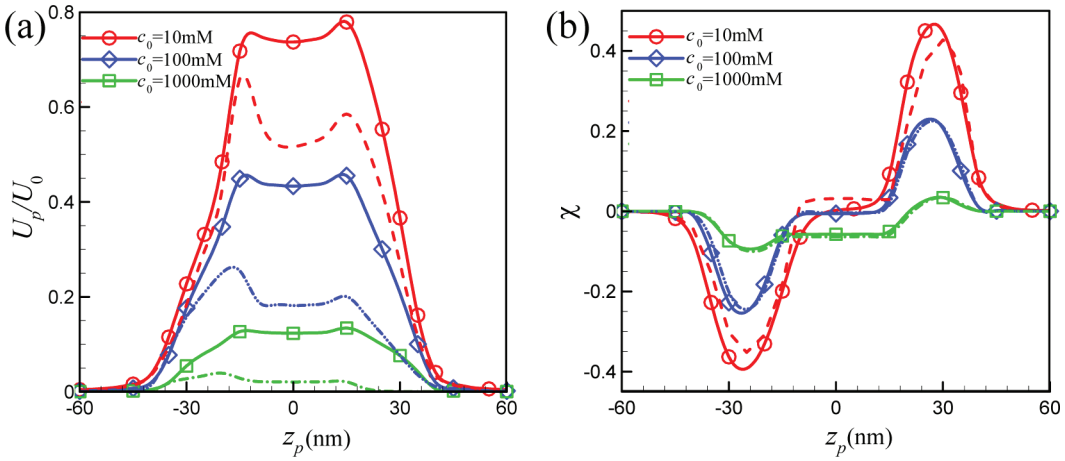

Figure 2. Normalized particle translation velocity (a) and ionic current deviation (b) as a function of the particle's location at various bulk ionic concentrations when $\rho_{fix} = -6 \times 10^7$ C/m^3, $\gamma = 1.32 \times 10^{18}$ kg/sm^3, $\sigma_w = 0$ C/m^2, and $E = 2000$ kV/m. Solid lines with circles, diamonds, and squares represent the results of $\varepsilon_{f,i} = \varepsilon_{f,o} = \varepsilon_w = 80$ at $C_0 = 10$, 100, and 1000 mM, respectively. Dashed, dash-double dotted, and dash-dotted lines represent the results with the LPE effect for $C_0 = 10$, 100, and 1000 mM, respectively.

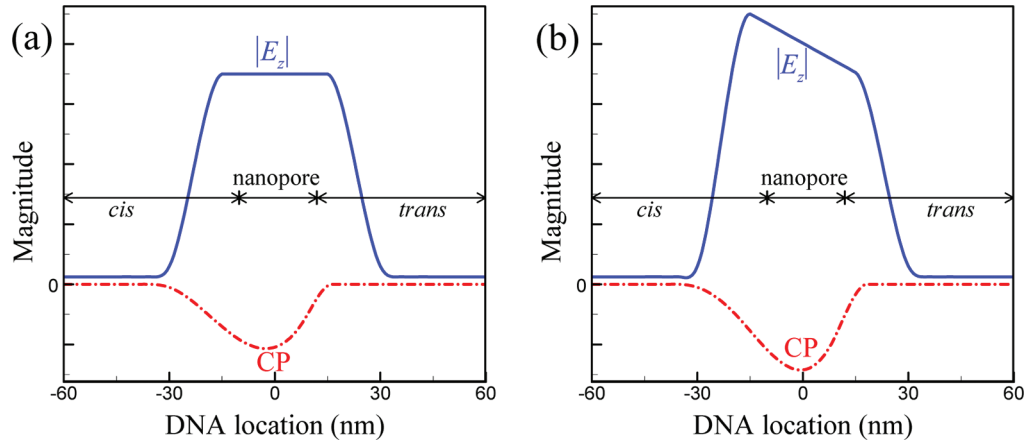

Figure 3. Qualitative description of the physical mechanisms of affecting the DNA translocation through a nanopore (not to actual scale). (a) $\varepsilon_{f,i} = \varepsilon_{f,o} = \varepsilon_w = 80$; (b) $\varepsilon_{f,i} = \varepsilon_i$ and $\varepsilon_{f,o} = \varepsilon_r$. $|E_z|$: local enhanced electric field. CP: concentration polarization.

and the nanopore wall and DNA–nanopore wall interactions, which include overlapping of the EDLs of the DNA nanoparticle and the charged nanopore wall, and compression of the EDL of the DNA nanoparticle by the nearby (un)charged nanopore wall. The CP effect results in more counterions accumulated near the entrance of the nanopore inside the *cis* reservoir. Figure 4 depicts the normalized ionic concentration difference between the cations and the anions, $c_1^* - c_2^* = (c_1 - c_2)/C_0$, when $z_p = -15.6$ (a, d), 0 (b, e), and 15.6 nm (c, f) in the absence (a–c) and presence (d–f) of the LPE effect. As expected, the spatial distribution of the net charge within the liquid, which is proportional to $c_1^* - c_2^*$, varies with the position of the nanoparticle. During the DNA translocation through the nanopore, the electroosmotic flow (EOF) in the gap between the particle and the nanopore wall, the direction of which is opposite to the particle electrophoretic motion, drives counterions from the nanopore toward the *cis* reservoir, leading to more counterions accumulated near the *cis* reservoir of the nanopore and resulting in a concentration gradient across the nanopore. Figure 4 also shows that CP with the LPE effect (Figure 4d–f) is more significant than that without considering the LPE effect as shown in Figure 4a–c. This is because the LPE effect leads to more counterions confined in the vicinity of the DNA surface, which reduces the electrostatic interaction between the DNA surface and the counterions flowing in the gap between the particle and the nanopore wall toward the *cis* reservoir. Therefore, counterions with the LPE effect are easier to pass through the nanopore toward the rear end of the DNA nanoparticle, leading to more significant CP effect than the case without the LPE effect. The induced CP effect generates an electric field, the direction of which is opposite to the externally imposed one, resulting in a decrease in the particle velocity. The local minimum of the particle translocation velocity occurring in the range of -15.6 nm $< z_p <$ 15.6 nm is mainly attributed to the CP effect. Since the CP effect becomes more significant when the LPE effect is considered, the particle velocity with the LPE effect has a more pronounced local minimum than that without considering the LPE effect, as shown in Figure 2a. Without considering the LPE effect, the presence of the two peak particle velocities at $z_p = \pm 15.6$ nm is mainly due to the CP effect, which is more significant when the particle is completely inside the nanopore since the axial electric field inside the nanopore is almost independent of the particle's location, as shown in Figure 5a and b. When the LPE effect is considered, the axial electric field inside the nanopore depends on the particle's location, as shown in Figure 5c,d. The

dx.doi.org/10.1021/jp211798x | J. Phys. Chem. C 2012, 116, 4793–4801

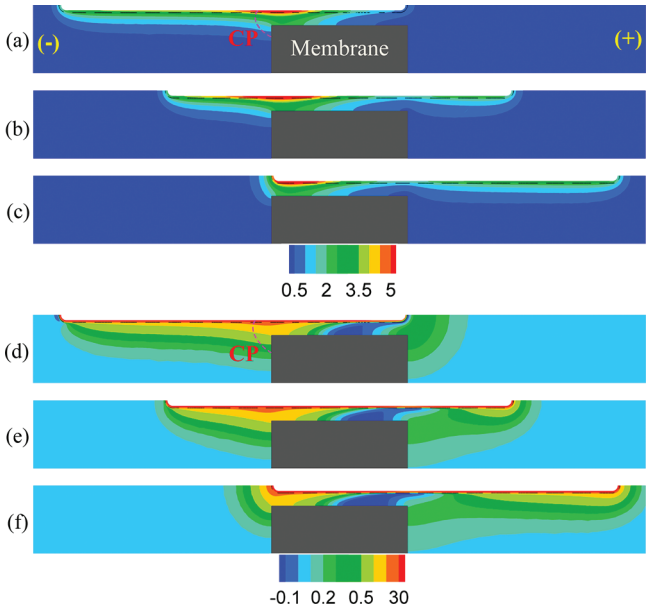

Figure 4. Spatial distribution of the normalized net ionic concentration difference, $(c_1 - c_2)/C_0$, at various particle locations in the absence (a–c) and presence (d–f) of the LPE effect for C_0 = 10 mM and z_p = −15.6 nm (a and d), 0 nm (b and e), and 15.6 nm (c and f).

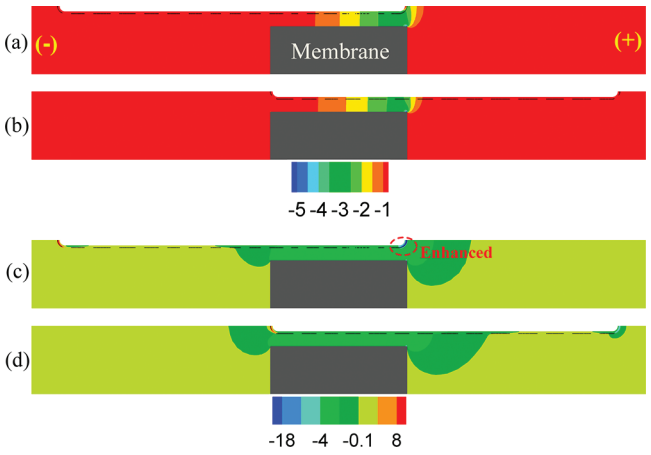

Figure 5. Spatial distribution of the normalized local axial electric field, $E_z^* = E_z/E_{ref}$ with $E_z = -dV/dz$ and $E_{ref} = RT/Fa$, at various particle locations in the absence (a and b) and presence (c and d) of the LPE effect for C_0 = 10 mM, z_p = −15.6 nm (a and c), and z_p = 15.6 nm (b and d).

average axial electric field inside the nanopore decreases as the particle translocates through the nanopore, which explains why the first peak particle velocity occurring when the particle completely enters the nanopore is higher than the second peak particle velocity when the rear end of the particle exits from the nanopore. In addition, the magnitude of the axial electric field in the presence of the LPE effect is much higher than that without the LPE effect. The significantly enhanced local electric field increases the flow inside the nanopore and accordingly brings more counterions toward the *cis* reservoir near the nanopore, resulting in more significant CP as shown in Figure 4. With the LPE effect, the asymmetric particle velocity profile in the range of -15.6 nm $< z_p <$ 15.6 nm is due to the combined competitive effects of the enhanced local electric field and the CP effect, as schematically shown in Figure 3b. Note that the mechanisms schematically shown in Figure 3 highly depend on the Debye length (EDL thickness). CP decreases as the bulk ionic concentration C_0 increases. Therefore, without the LPE effect the particle velocity inside the nanopore is nearly a constant when the bulk concentration is relatively high (i.e., C_0 = 1000 mM in Figure 2a). With the LPE effect, the particle velocity inside the nanopore is not a constant even when the bulk ionic concentration is relatively high, and this is due to the dependence of the axial electric field on the particle position, as shown in Figure 5.

In general, the nanopore-based sensing technique is based on the variation of the ionic current through the nanopore due to the presence of the particle. The influence of the DNA nanoparticle's location on the ionic current deviation through the nanopore is shown in Figure 2b. The current deviations in the absence (solid lines with symbols) and presence (lines without symbols) of the LPE effect are almost identical for C_0 = 100 and 1000 mM, and their trends are very similar for C_0 = 10 mM, implying that the LPE effect on the ionic current deviation is insignificant under the conditions considered. Figure 2b also reveals that a current blockade is observed as the DNA enters the nanopore, and current enhancement occurs as the DNA starts to exit the nanopore. It is generally accepted that the former arises from the physical blocking by the DNA nanoparticle, which is consistent with many experimental results in the literature.[4,6,14−18] The latter was also observed by many groups.[11,12,21,22,25,30,32,51] For example, Chang et al.[11] experimentally studied electrokinetic translocation of a 200 bp dsDNA through a silica nanopore of 2.2 nm in radius and 50 nm in length, and its geometry is very similar to our simulation. They found that if the DNA molecule is about the same length of the nanopore current enhancement occurs and is attributed to additional counterions (cations) carried by the negatively charged DNA into the nanopore. Liu et al.[25] attribute the current enhancement to the positive diffusive current, and this occurs only under the conditions of a thick EDL and a high electric field externally imposed. The initial current blockade as the DNA enters the nanopore is mainly due to the displacement of electrolyte solution out of the nanopore by the DNA nanoparticle. The negatively charged DNA also brought some counterions into the nanopore, as shown in Figure 4, leading to an increase in the ionic conductance and consequently current enhancement. The current enhancement appears as the DNA completely enters the nanopore and attains the maximum as the DNA starts exiting from the nanopore.

3.2. Effect of the Strength of the Applied Electric Field. Figure 6 depicts the translational velocity and the ionic current deviation as a function of the particle's location at various bulk ionic concentrations when the applied electric field is E = 20 kV/m, which is 1/100 times that in Figure 2. To compare the results for both E = 20 and 2000 kV/m, the y-axis in Figure 6a is multiplied by 100. Comparison between Figures 2a and 6a reveals that under the same other conditions the particle translocation velocity for E = 2000 kV/m is nearly 100 times of that for E = 20 kV/m. Without considering the LPE effect, the particle velocity profile for E = 20 kV/m is very similar to that for E = 2000 kV/m shown in Figure 2a. However, with the LPE effect, the particle velocity when the rear end of the particle just exits the nanopore (i.e., z_p = 15.6 nm) is higher than that when the front end of the DNA just enters the nanopore (z_p = −15.6 nm), which is different from the results shown in Figure 2a. Figure 6a also reveals that the higher the bulk ionic concentration the lower the particle

dx.doi.org/10.1021/jp211798x | J. Phys. Chem. C 2012, 116, 4793−4801

translocation velocity, which is consistent with the results in Figure 2a. However, when the bulk ionic concentration is sufficiently low (i.e., C_0 = 10 mM) and E = 20 kV/m, the particle velocity becomes negative prior to entering the nanopore, implying that the DNA is trapped near the entrance of the nanopore, which has also been found in some experimental results.[52,53] Since the particle could not translocate through the nanopore, we did not plot the results for C_0 = 10 mM in Figure 6. The particle trapping is because the electrophoretic driving force is not high enough to overcome the net effects of the entropic costs of squeezing a coil polyelectrolyte into a narrow pore[6] and the opposite electroosmotic flow coming from the charged particle.[28,29]

Figure 6b depicts the ionic current deviation during the particle translocation process when E = 20 kV/m. When the bulk ionic concentration is sufficiently high (i.e., 1000 mM), the current blockade happens during the entire translocation process for both the absence and presence of the LPE effect, and the LPE effect on the current deviation is insignificant. However, for the bulk concentration C_0 = 100 mM, a current blockade is observed when the LPE effect is not considered, while both the current blockade and enhancement are found when the LPE effect is taken into account. The current blockade and enhancement behavior at relatively low electric field can be attributed to more counterions, which are accumulated surrounding the DNA surface due to the counterion condensation, and are carried into the nanopore.

3.3. Effect of the Surface Charge of the Nanopore. In practical applications, the nanopore wall usually carries a negative surface charge arising from the dissociation of functional groups on it, such as the negatively charged groups, Si−O$^-$, dissociated from the silanol groups on the silica nanopore wall. Consequently, an extra electroosmotic flow (EOF) will be induced near the charged nanopore wall, which in turn affects both the ionic current and the particle translocation through the nanopore.[54] Figure 7a shows the influence of the nanopore surface charge density, σ_w, on the translational velocity of the DNA. In this case, σ_w is assumed to be −0.009 C/m^2.[25] As expected, the negatively charged nanopore induces an EOF, the direction of which is opposite to that of the DNA electrophoretic motion. Therefore, the DNA translational velocity for σ_w = −0.009 C/m^2 is lower than that in an uncharged

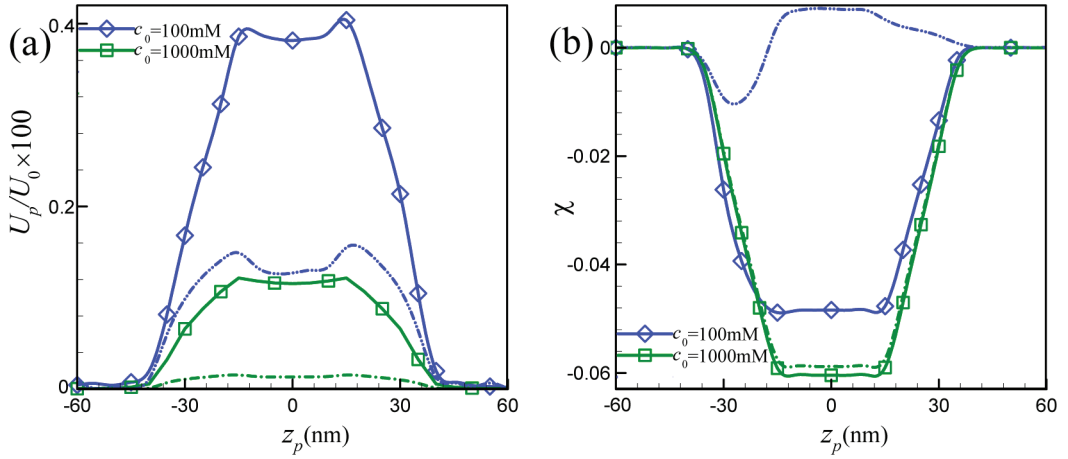

Figure 6. Normalized particle translation velocity (a) and ionic current deviation (b) as a function of the particle's location when ρ_{fix} = −6 × 10^7 C/m^3, γ = 1.32 × 10^{18} kg/sm^3, σ_w = 0 C/m^2, and E = 20 kV/m. Solid lines with diamonds and squares represent the results without considering the LPE effect at C_0= 100 and 1000 mM, respectively. Dash-double dotted and dash-dotted lines represent the results with the LPE effect at C_0= 100 and 1000 mM, respectively.

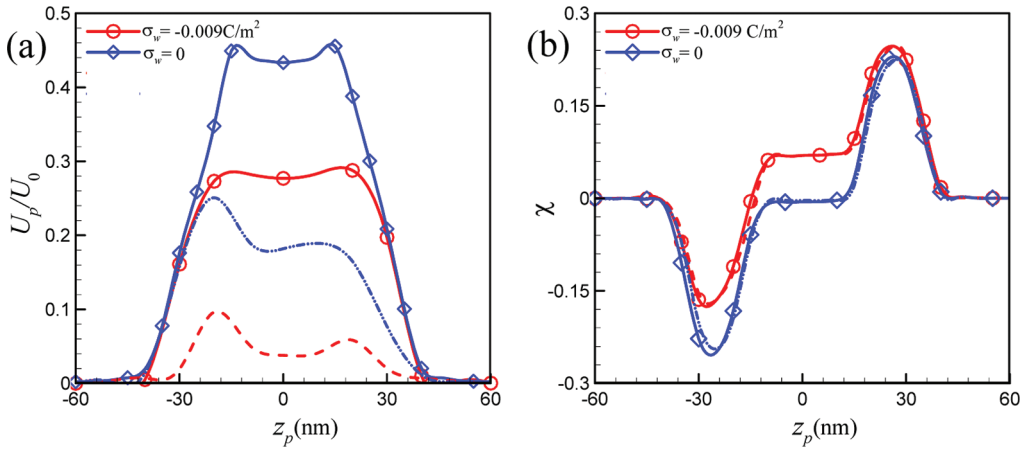

Figure 7. Influence of the nanopore surface charge density σ_w on the normalized particle translation velocity (a) and ionic current deviation (b) when C_0 = 100 mM, ρ_{fix} = −6 × 10^7 C/m^3, γ = 1.32 × 10^{18} kg/sm^3, and E = 2000 kV/m. Solid lines with circles and diamonds represent the reference results without the LPE effect at σ_w = −0.009 C/m^2 and σ_w = 0 C/m^2, respectively. Dashed and dash-double dotted lines represent the results with the LPE effect at σ_w = −0.009 C/m^2 and σ_w = 0 C/m^2, respectively.

dx.doi.org/10.1021/jp211798x | J. Phys. Chem. C 2012, 116, 4793−4801

nanopore. The LPE effects in both charged and uncharged nanopores are similar, as shown in Figure 7a. We further examine the influence of the nanopore surface charge density on the ionic current deviation, as shown in Figure 7b. The same as that in an uncharged nanopore, the LPE effect is not significant in a charged nanopore. Both current blockade and enhancement are observed in both uncharged and charged nanopores. However, the current enhancement phenomenon in a charged nanopore becomes more significant than that in an uncharged nanopore, and this is because there are more counterions in the negatively charged nanopore, yielding an increase in the ionic current. Note that the predicted behaviors of the ionic current are quite consistent with the experiments of sensing single molecule by nanopores,[12] where both current blockade and enhancement behaviors have been observed: the typical phenomenon of the former often appears in high salt concentration, while the latter is usually observed under the conditions of relatively low salt concentration.[11,12,30,51]

To further understand the dependence of the ionic current on the salt concentration during the DNA translocation process, we define a relative ionic current when the DNA is at the center of the nanopore, $\chi_0 = (I_0 - I_\infty)/I_\infty$,[30] where I_0 is the ionic current when the DNA is at the center of the nanopore (i.e., $z_p = 0$). Figure 8 shows χ_0 as a function of the salt concentration under two different electric fields imposed. When the applied electric field is relatively high (i.e., $E = 2000$ kV/m), the LPE effect on the relative ionic current χ_0 is insignificant. Current enhancement occurs when C_0 is below a critical value, which is about 300 mM under the considered conditions, and the current blockade is predicted when C_0 is above the critical salt concentration. This is in good qualitative agreement with the experimental observations.[12] When the applied electric field is reduced 10 times (i.e., $E = 200$ kV/m), both current blockade and enhancement are observed when the LPE effect is considered, while only the current blockade is observed when the LPE effect is not considered. The former qualitatively agrees with the theoretical results and experimental observations,[12] while the latter failed to predict the current enhancement phenomenon.

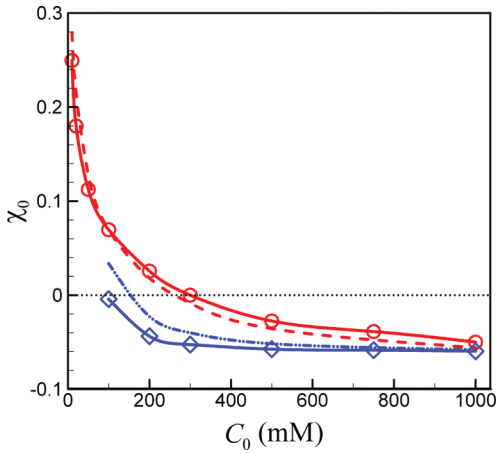

Figure 8. Relative ionic current due to the presence of the DNA at the nanopore's center as a function of the bulk ionic concentration when $\rho_{fix} = -6 \times 10^7$ C/m^3, $\gamma = 1.32 \times 10^{18}$ kg/sm^3, and $\sigma_w = -0.009$ C/m^2. Solid lines with circles and diamonds represent the reference results without the LPE effect at $E = 2000$ kV/m and $E = 200$ kV/m, respectively. Dashed and dash-double dotted lines represent the results with the LPE effect at $E = 2000$ kV/m and $E = 200$ kV/m, respectively.

Therefore, the LPE effect considered here is very important during the DNA translocation through the nanopore, especially when the electric field imposed is relatively low.

4. CONCLUSIONS

We have theoretically investigated for the first time the influence of the local liquid permittivity surrounding the DNA nanoparticle on the DNA electrokinetic translocation through a nanopore. Compared to the typical assumption of a uniform permittivity, the spatially varying permittivity in the vicinity of the DNA is more realistic because of counterion condensation and/or the strong hydrogen bonding interactions in the vicinity of a DNA molecule. We proposed two important mechanisms, local electric field enhancement and concentration polarization, to explain why the DNA translocation velocity profiles with and without the LPE effect are distinctly different. The LPE effect in general reduces the particle translocation velocity. Its effect on the ionic current deviation is insignificant when the applied electric field is relatively high. However, when the applied electric field is relatively low, both current blockade and current enhancement are predicted at relatively low salt concentration if the LPE effect is considered, while only the current blockade is found otherwise. Taking the LPE effect into account, the dependence of the ionic current on the salt concentration is in better agreement with the existing experimental observations.

■ ASSOCIATED CONTENT

Ⓢ Supporting Information

Details of the numerical implementation and code validation of the present study and the results of the effect of the hydrodynamic friction coefficient of the ion-penetrable layer on the particle translation velocity. This material is available free of charge via the Internet at http://pubs.acs.org.

■ AUTHOR INFORMATION

Corresponding Author

*E-mail: sqian@odu.edu (Shizhi Qian); jphsu@ntu.edu.tw (Jyh-Ping Hsu).

Author Contributions

‖These two authors contributed equally to this work.

Notes

The authors declare no competing financial interest.

■ ACKNOWLEDGMENTS

This work was funded, in part, by the Korea Institute of Machinery & Materials (KIMM), the World Class University Grant No. R32-2008-000-20082-0 of the National Research Foundation of Korea, and the National Science Council of the Republic of China.

■ REFERENCES

(1) Dekker, C. *Nat. Nanotechnol.* **2007**, *2*, 209−215.
(2) Talaga, D. S.; Li, J. L. *J. Am. Chem. Soc.* **2009**, *131*, 9287−9297.
(3) Han, A.; Creus, M.; Schurmann, G.; Linder, V.; Ward, T. R.; de Rooij, N. F.; Staufer, U. *Anal. Chem.* **2008**, *80*, 4651−4658.
(4) Venkatesan, B. M.; Bashir, R. *Nat. Nanotechnol.* **2011**, *6*, 615−624.
(5) Li, J. L.; Gershow, M.; Stein, D.; Brandin, E.; Golovchenko, J. A. *Nat. Mater.* **2003**, *2*, 611−615.
(6) Howorka, S.; Siwy, Z. *Chem. Soc. Rev.* **2009**, *38*, 2360−2384.
(7) Meller, A.; Nivon, L.; Brandin, E.; Golovchenko, J.; Branton, D. *Proc. Natl. Acad. Sci. U.S.A.* **2000**, *97*, 1079−1084.

(8) Branton, D.; Deamer, D. W.; Marziali, A.; Bayley, H.; Benner, S. A.; Butler, T.; Di Ventra, M.; Garaj, S.; Hibbs, A.; Huang, X. H.; Jovanovich, S. B.; Krstic, P. S.; Lindsay, S.; Ling, X. S. S.; Mastrangelo, C. H.; Meller, A.; Oliver, J. S.; Pershin, Y. V.; Ramsey, J. M.; Riehn, R.; Soni, G. V.; Tabard-Cossa, V.; Wanunu, M.; Wiggin, M.; Schloss, J. A. *Nat. Biotechnol.* **2008**, *26*, 1146−1153.
(9) Tsutsui, M.; Taniguchi, M.; Yokota, K.; Kawai, T. *Nat. Nanotechnol.* **2010**, *5*, 286−290.
(10) Meller, A.; Nivon, L.; Branton, D. *Phys. Rev. Lett.* **2001**, *86*, 3435−3438.
(11) Chang, H.; Kosari, F.; Andreadakis, G.; Alam, M. A.; Vasmatzis, G.; Bashir, R. *Nano Lett.* **2004**, *4*, 1551−1556.
(12) Smeets, R. M. M.; Keyser, U. F.; Krapf, D.; Wu, M. Y.; Dekker, N. H.; Dekker, C. *Nano Lett.* **2006**, *6*, 89−95.
(13) Iqbal, S. M.; Akin, D.; Bashir, R. *Nat. Nanotechnol.* **2007**, *2*, 243−248.
(14) Chen, Z.; Jiang, Y. B.; Dunphy, D. R.; Adams, D. P.; Hodges, C.; Liu, N. G.; Zhang, N.; Xomeritakis, G.; Jin, X. Z.; Aluru, N. R.; Gaik, S. J.; Hillhouse, H. W.; Brinker, C. J. *Nat. Mater.* **2010**, *9*, 667−675.
(15) Wanunu, M.; Morrison, W.; Rabin, Y.; Grosberg, A. Y.; Meller, A. *Nat. Nanotechnol.* **2010**, *5*, 160−165.
(16) Schneider, G. F.; Kowalczyk, S. W.; Calado, V. E.; Pandraud, G.; Zandbergen, H. W.; Vandersypen, L. M. K.; Dekker, C. *Nano Lett.* **2010**, *10*, 3163−3167.
(17) Venkatesan, B. M.; Shah, A. B.; Zuo, J. M.; Bashir, R. *Adv. Funct. Mater.* **2010**, *20*, 1266−1275.
(18) Min, S. K.; Kim, W. Y.; Cho, Y.; Kim, K. S. *Nat. Nanotechnol.* **2011**, *6*, 162−165.
(19) Firnkes, M.; Pedone, D.; Knezevic, J.; Doblinger, M.; Rant, U. *Nano Lett.* **2010**, *10*, 2162−2167.
(20) Storm, A. J.; Storm, C.; Chen, J. H.; Zandbergen, H.; Joanny, J. F.; Dekker, C. *Nano Lett.* **2005**, *5*, 1193−1197.
(21) Aksimentiev, A.; Heng, J. B.; Timp, G.; Schulten, K. *Biophys. J.* **2004**, *87*, 2086−2097.
(22) Heng, J. B.; Ho, C.; Kim, T.; Timp, R.; Aksimentiev, A.; Grinkova, Y. V.; Sligar, S.; Schulten, K.; Timp, G. *Biophys. J.* **2004**, *87*, 2905−2911.
(23) Muthukumar, M.; Kong, C. Y. *Proc. Natl. Acad. Sci. U.S.A.* **2006**, *103*, 5273−5278.
(24) Ghosal, S. *Phys. Rev. Lett.* **2007**, *98*, 238104.
(25) Liu, H.; Qian, S. Z.; Bau, H. H. *Biophys. J.* **2007**, *92*, 1164−1177.
(26) van Dorp, S.; Keyser, U. F.; Dekker, N. H.; Dekker, C.; Lemay, S. G. *Nat. Phys.* **2009**, *5*, 347−351.
(27) Ai, Y.; Liu, J.; Zhang, B. K.; Qian, S. *Anal. Chem.* **2010**, *82*, 8217−8225.
(28) Ai, Y.; Qian, S. Z. *Phys. Chem. Chem. Phys.* **2011**, *13*, 4060−4071.
(29) Zhang, M. K.; Ai, Y.; Sharma, A.; Joo, S. W.; Kim, D. S.; Qian, S. Z. *Electrophoresis* **2011**, *32*, 1864−1874.
(30) He, Y. H.; Tsutsui, M.; Fan, C.; Taniguchi, M.; Kawai, T. *ACS Nano* **2011**, *5*, 5509−5518.
(31) He, Y. H.; Tsutsui, M.; Fan, C.; Taniguchi, M.; Kawai, T. *ACS Nano* **2011**, *5*, 8391−8397.
(32) Fan, R.; Karnik, R.; Yue, M.; Li, D. Y.; Majumdar, A.; Yang, P. D. *Nano Lett.* **2005**, *5*, 1633−1637.
(33) Honig, B.; Nicholls, A. *Science* **1995**, *268*, 1144−1149.
(34) Ramstein, J.; Lavery, R. *Proc. Natl. Acad. Sci. U.S.A.* **1988**, *85*, 7231−7235.
(35) Young, M. A.; Jayaram, B.; Beveridge, D. L. *J. Phys. Chem. B* **1998**, *102*, 7666−7669.
(36) Malysheva, O.; Tang, T.; Schiavone, P. *J. Phys. Chem. C* **2010**, *114*, 3781−3790.
(37) Cui, S. T. *J. Phys. Chem. B* **2011**, *115*, 10699−10706.
(38) Ohshima, H. *Adv. Colloid Interface Sci.* **1995**, *62*, 189−235.
(39) Yeh, L. H.; Hsu, J. P.; Tseng, S. *J. Phys. Chem. C* **2010**, *114*, 16576−16587.
(40) Zhang, M. K.; Ai, Y.; Kim, D. S.; Jeong, J. H.; Joo, S. W.; Qian, S. Z. *Colloid Surf., B* **2011**, *88*, 165−174.
(41) Yeh, L. H.; Hsu, J. P. *Soft Matter* **2011**, *7*, 396−411.
(42) Keh, H. J.; Anderson, J. L. *J. Fluid Mech.* **1985**, *153*, 417−439.
(43) Holt, J. K.; Park, H. G.; Wang, Y. M.; Stadermann, M.; Artyukhin, A. B.; Grigoropoulos, C. P.; Noy, A.; Bakajin, O. *Science* **2006**, *312*, 1034−1037.
(44) Trifonov, E. N.; Sussman, J. L. *Proc. Natl. Acad. Sci. U.S.A.* **1980**, *77*, 3816−3820.
(45) Spiering, A.; Getfert, S.; Sischka, A.; Reimann, P.; Anselmetti, D. *Nano Lett.* **2011**, *11*, 2978−2982.
(46) Manning, G. S. *J. Chem. Phys.* **1969**, *51*, 924−933.
(47) Keyser, U. F.; van Dorp, S.; Lemay, S. G. *Chem. Soc. Rev.* **2010**, *39*, 939−947.
(48) Muthukumar, M. *J. Chem. Phys.* **2004**, *120*, 9343−9350.
(49) Stein, D.; Deurvorst, Z.; van der Heyden, F. H. J.; Koopmans, W. J. A.; Gabel, A.; Dekker, C. *Nano Lett.* **2010**, *10*, 765−772.
(50) Cheng, L. J.; Guo, L. J. *Chem. Soc. Rev.* **2010**, *39*, 923−938.
(51) Aksimentiev, A. *Nanoscale* **2010**, *2*, 468−483.
(52) Plecis, A.; Schoch, R. B.; Renaud, P. *Nano Lett.* **2005**, *5*, 1147−1155.
(53) Wang, Y. C.; Stevens, A. L.; Han, J. Y. *Anal. Chem.* **2005**, *77*, 4293−4299.
(54) Stein, D.; Kruithof, M.; Dekker, C. *Phys. Rev. Lett.* **2004**, *93*, 035901.